










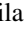




Lifetime measurements of low-lying states in odd-mass isotopes $^{117,119}\text{Te}$ and the nature of vibration in Te isotopes

E. A. Cederlöf ^{1,2,*}, T. Bäck ¹, J. Nyberg ², C. Qi ¹, A. Ataç ¹, T. Braunroth ^{3,†}, T. Calverley ⁴, D. M. Cox ⁴, M. Doncel ^{5,‡}, T. Grahn ⁴, P. Greenlees ⁴, J. Hilton ⁴, R. Julin ⁴, J. Konki ⁴, H. Li ⁶, V. Modamio ⁷, B. S. Nara Singh ^{8,§}, J. Pakarinen ⁴, P. Papadakis ^{4,||}, J. Partanen ⁴, P. Rahkila ⁴, P. Ruotsalainen ⁴, M. Sandzelius ⁴, J. Sarén ⁴, C. Scholey ⁴, S. Stolze ⁴, P. Subramaniam ¹, W. Teng ⁹, J. Uusitalo ⁴, J. J. Valiente-Dobón ¹⁰ and Y. Zhang ⁹

¹Department of Physics, KTH Royal Institute of Technology, SE-10691 Stockholm, Sweden

²Department of Physics and Astronomy, Uppsala University, SE-75120 Uppsala, Sweden

³Institut für Kernphysik, Universität zu Köln, 50937 Köln, Germany

⁴Accelerator Laboratory, Department of Physics, University of Jyväskylä, FI-40014 Jyväskylä, Finland

⁵Departamento de Física Fundamental, University of Salamanca, E-37008 Salamanca, Spain

⁶Grand Accélérateur National d'Ions Lourds, CEA/DRF-CNRS/IN2P3, Boîte Postale 55027, 14076 Caen cedex 5, France

⁷Department of Physics, University of Oslo, NO-0316 Oslo, Norway

⁸School of Physics and Astronomy, The University of Manchester, Manchester M13 9PL, United Kingdom

⁹Department of Physics, Liaoning Normal University, Dalian 116029, People's Republic of China

¹⁰INFN, Laboratori Nazionali di Legnaro, Legnaro, Italy



(Received 15 February 2025; accepted 1 July 2025; published 21 July 2025)

Background: With the recent lifetime measurements of the 2^+ states in ^{116}Te and ^{118}Te , the evolution of the collectivity in the midshell region of the Te isotopic chain is starting to reveal itself. However, more information on the structure of the ground-state bands and the nature of the collectivity can be gathered from studying the odd-mass systems, in which lifetimes have not been extensively studied.

Purpose: The purpose of the present work is to investigate the structure of low-lying excited states of the $\nu h_{11/2}$ band in the odd-mass systems ^{117}Te and ^{119}Te , that correspond to the ground-state band in even-even Te.

Methods: Lifetimes of low-lying states in the $\nu h_{11/2}$ band of ^{117}Te are measured for the first time and remeasured in ^{119}Te , using the recoil distance Doppler shift technique, and analyzed with the differential decay curve method in coincidence mode.

Results: The lifetimes and $B(E2)$ values of the first two transitions, $15/2^- \rightarrow 11/2^-$ and $19/2^- \rightarrow 15/2^-$, in the $\nu h_{11/2}$ band, are determined in both ^{117}Te and ^{119}Te . From the lifetimes, the $B(E2)$ values and corresponding $B_{4/2}$ ratios are determined. The results are compared to systematics in both even- A and odd- A Te isotopes, as well as with theoretical results from the large-scale shell model and interacting boson model calculations.

Conclusions: While the energy levels of ^{117}Te and ^{119}Te , similarly to ^{118}Te , exhibit textbook vibrational behavior, the unexpectedly small $B_{4/2}$ ratios of these odd-mass nuclei point to a puzzling discrepancy and question the vibrational nature of these states.

DOI: [10.1103/fmgd-tj4w](https://doi.org/10.1103/fmgd-tj4w)

I. INTRODUCTION

The collectivity in the isotopic chains of tellurium ($Z = 52$) and cadmium ($Z = 48$) have long been of particular interest as they are expected to be the ideal testing ground for understanding the nature of quantum vibration in atomic nuclei [1]. Indeed, the yrast bands of many midshell region Cd and Te isotopes show perfectly vibrational-like behavior, accompanied by the appearance of low-lying, low-spin states expected as multiphonon excitations. Recent studies, however, start to cast doubt on the vibrational nature of these states [2–5]. Thus more eyes have turned towards the midshell region, with new lifetime measurements in ^{116}Te [6,7] and ^{118}Te [7,8], where a shape phase transition from prolate to oblate deformation is expected [5].

Vibration, and quadrupole collectivity in general, is commonly studied in the yrast states and the connecting E2 electromagnetic transitions. It can, in particular, be

* Contact author: ebbace@kth.se

† Present address: Gesellschaft für Anlagen und Reaktorsicherheit (GRS) GmbH, Köln, Germany.

‡ Present address: Department of Physics, Stockholm University, SE-10691 Stockholm, Sweden.

§ Present address: School of Computing Engineering and Physical Sciences, University of the West of Scotland, Paisley PA1 2BE, United Kingdom.

|| Present address: STFC Daresbury Laboratory, Warrington WA4 4AD, United Kingdom.

Published by the American Physical Society under the terms of the [Creative Commons Attribution 4.0 International](https://creativecommons.org/licenses/by/4.0/) license. Further distribution of this work must maintain attribution to the author(s) and the published article's title, journal citation, and DOI. Funded by [Bibsam](https://www.bibsam.com/).

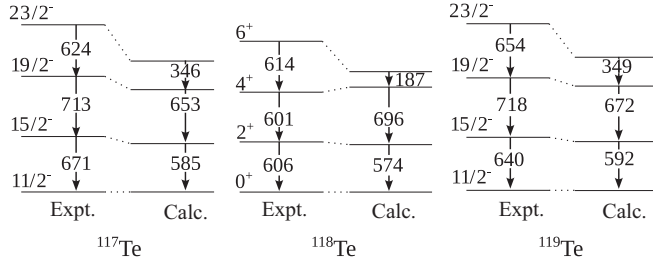


FIG. 1. Partial level schemes for $^{117-119}\text{Te}$: experimental values and comparison to shell model calculations.

probed through observables such as the energy level ratio, $E_{4/2}$, and the reduced transition probability ratio, $B_{4/2}$, here defined in the following way to allow for both odd- and even-mass nuclei: $E_{4/2} \equiv (E_{J+4} - E_J)/(E_{J+2} - E_J)$ and $B_{4/2} = B(E2; J+4 \rightarrow J+2)/B(E2; J+2 \rightarrow J)$, where J is the spin of the band head. In the vibrational limit, $E_{4/2} = 2$ and $B_{4/2} = 2$, while in the rotational limit $E_{4/2} = 3.33$ and $B_{4/2} = 1.43$ [9].

While the $B(E2)$ values have mostly been studied in the ground-state bands of the even-mass Te nuclei, the neighboring odd-mass nuclei may also contain important information on the nature of the ground-state band. In the odd-mass Te isotopes, the yrast $23/2^-$, $19/2^-$, and $15/2^-$ states have been interpreted as being due to the coupling of an $h_{11/2}$ neutron to the 6^+ , 4^+ , and 2^+ states in the neighboring even-mass Te core. The odd-mass systems thus provide further information on the evolution of the shell structure of these bands, and in particular the effect of the unpaired neutron. While the transition strengths now are known for the ground-state transitions in all even-mass Te nuclei ranging from $N = 56$ up to the shell closure at $N = 82$ (and beyond), experimental data are still missing in the $\nu h_{11/2}$ band for a majority of the odd-mass Te isotopes. Before this work, lifetimes of the yrast $15/2^-$ and $19/2^-$ states have only been measured in the odd-mass Te nuclei ^{109}Te [10] and ^{119}Te [11]. In this work lifetime measurements in ^{117}Te will be presented for the first time, as well as a remeasurement of the lifetimes in ^{119}Te .

Excited states in ^{117}Te and ^{119}Te , the odd-mass neighbors of ^{116}Te and ^{118}Te , have previously been determined up to high spin in Refs. [12,13]. Partial level schemes of the two odd-mass nuclei and ^{118}Te , presented in Fig. 1 together with shell model calculations that will be presented in the discussion, show that the structure of the odd-parity bands built on the $11/2^-$ band head is similar to the vibrational-like bands in ^{118}Te . In this work, reduced transition probabilities of the $19/2^- \rightarrow 15/2^-$ and $15/2^- \rightarrow 11/2^-$ transitions in ^{117}Te and ^{119}Te , analogous to the $4^+ \rightarrow 2^+$ and $2^+ \rightarrow 0^+$ transitions in the even-even neighbors, are determined through lifetime measurements. It will be shown that, while the spectra of these odd-mass nuclei are nearly identical to that of ^{118}Te , with $E_{4/2}$ close to the vibrational limit, the measured $B_{4/2}$ ratio tentatively suggests a different behavior. The results are compared with large-scale shell model (LSSM) and interacting boson model (IBM) calculations.

II. EXPERIMENTAL DETAILS

A plunger experiment measuring lifetimes of excited states in ^{117}Te and ^{119}Te utilizing the recoil distance Doppler-shift (RDDS) technique [14,15] was carried out at the JYFL accelerator laboratory in Jyväskylä, Finland, in 2017, using the DPUNS plunger [16] coupled to the Jurogam II γ -ray spectrometer [17–19]. In the RDDS technique, a recoil produced via a beam-induced reaction at the target position travels towards a thick stopper foil. The recoil may either decay in flight, in which case the energy of the transition will be Doppler shifted, or it may decay at rest in the stopper, in which case the energy will be unshifted. Lifetime information is gathered by the change in intensity of the unshifted and shifted peaks as the target-to-stopper distance x is varied.

The excited states were populated in the fusion-evaporation reactions $^{100}\text{Mo}(^{22}\text{Ne}, 5n)^{117}\text{Te}$ and $^{100}\text{Mo}(^{22}\text{Ne}, 3n)^{119}\text{Te}$, at a beam energy of 75 MeV and a beam current of 4 pA. The beam energy was optimized for the production of ^{118}Te , and the result of the analysis of that nucleus is published in Ref. [8]. The population of the $15/2^-$ states in ^{117}Te and ^{119}Te was approximately 9% and 10%, respectively, compared to the population of the 2^+ state in ^{118}Te .

The target-to-stopper distance x was controlled using the DPUNS plunger, with a movable ^{100}Mo target of 0.68 mg/cm^2 thickness mounted together with an Au stopper foil of thickness 8 mg/cm^2 . Measurements were taken at eight different target-to-stopper distances, ranging from $x = 25$ to $215 \mu\text{m}$. With the mean velocity of the traveling recoils determined to be $v/c = 1.31(1)\%$ for ^{117}Te and $v/c = 1.34(1)\%$ for ^{119}Te , this corresponds to time of flights ranging from 6 to 55 ps.

The γ rays were detected using the Jurogam II γ -ray spectrometer. Jurogam II comprises 15 Compton suppressed Eurogam phase-1 Ge detectors and 24 Compton suppressed Eurogam Ge clover detectors arranged into four rings. Ring 1 contains five of the phase-1 detectors positioned at an angle of 157.6° relative to the beam axis, ring 2 contains ten of the phase-1 detectors at 133.6° , and rings 3 and 4 contain 12 clover detectors each, positioned at 104.5° and 75.5° , respectively. Throughout this paper, these rings will be referred to as R1–R4.

III. DATA ANALYSIS AND RESULTS

Data were collected and sorted into 32 $\gamma\gamma$ coincidence matrices using the GRAIN software package [20], corresponding to the four ring combinations R1 vs R1, R2 vs R2, R1 vs R2, and R2 vs R1 at the eight target-to-stopper distances. The $\gamma\gamma$ coincidence matrices will be denoted (RX, RY) , where the gate is set on ring RX and the fit is done in the projection in ring RY. Rings R3 and R4 were not used in the analysis, due to their angles being close to 90° and therefore experiencing a small Doppler shift, resulting in a small separation of the unshifted and shifted peaks.

A. Lifetimes of ^{117}Te

The lifetimes of the yrast $15/2^-$ and $19/2^-$ states were extracted using the differential decay curve method (DDCM)

[15,21] in coincidence mode with a gate on a direct feeding transition populating the state. The lifetime τ at each distance x can then be calculated according to DDCM in the following way:

$$\tau(x) = \frac{\{B_s, A_u\}(x)}{\frac{d}{dx}\{B_s, A_s\}(x)} \frac{1}{v}, \quad (1)$$

where v represents the mean recoil velocity and the notation $\{B, A\}$ signifies the intensity of the depopulating transition A when gating on the direct feeding transition B . The subscripts denote the Doppler-shifted (s) and unshifted (u) components of the transition. In the case of the $15/2^-$ state lifetime, the gate was set on the $19/2^- \rightarrow 15/2^-$ transition. Similarly, in the case of the $19/2^-$ state, the gate was set on the $23/2^- \rightarrow 19/2^-$ transition.

Before the fit of the peaks A_u and A_s could be done, a background subtraction was made by carefully selecting a gate on the Compton continuum close to the peak gate, making sure that it did not contain any photopeaks in coincidence with the transition of interest. The same gate position was used for all distances.

The fit of the unshifted and shifted components of the $15/2^-$ state in the background-subtracted projection was performed in all four matrix combinations of $R1$ and $R2$ and for all eight target-to-stopper distances. In the case of the $19/2^-$ state, however, in order to gain more statistics, the background-subtracted and gated spectra resulting from the matrices $(R2, R2)$ and $(R1, R2)$ were first summed, before performing the fit of the $19/2^-$ state in $R2$. Equivalently, the fit was also done in $R1$ after summing the gated and background-subtracted matrices $(R1, R1)$ and $(R2, R1)$. During the fit, the position and widths of the peaks were kept fixed for each ring. Examples of the fits are presented in Fig. 2 for both the $15/2^-$ and the $19/2^-$ states.

The intensities at each distance were normalized using the same normalization constants as were used in the previous analysis, from the same experiment, of ^{118}Te in Ref. [8]. In that paper, it is argued that the effect of deorientation on the normalization constants is negligible in this analysis.

Finally, the derivative of $\{B_s, A_s\}(x)$ was determined by fitting a series of piecewise continuously differentiable second-degree polynomials to the curve, using the NAPATAU [22] software. The lifetime was calculated according to Eq. (1) at each point x within the region of sensitivity, which is the region where the derivative of $\{B_s, A_s\}(x)$ is larger than half of its maximum. The final lifetime is calculated as the weighted average of these values. Examples of the results for the $15/2^-$ and $19/2^-$ states are presented in Fig. 3.

B. Lifetimes of ^{119}Te

The lifetime of the $19/2^-$ state in ^{119}Te was determined in the same way as for ^{117}Te , using Eq. (1) with a gate on the direct feeding transition $23/2^- \rightarrow 19/2^-$. However, the lifetime of the $15/2^-$ state could not be determined using this method due to the 718 keV doublets in ^{119}Te (not shown in Fig. 1), making the choice of a direct gate on the $19/2^- \rightarrow 15/2^-$ transition impossible. Instead, DDCM using an indirect gate was implemented, where the lifetime is calculated using

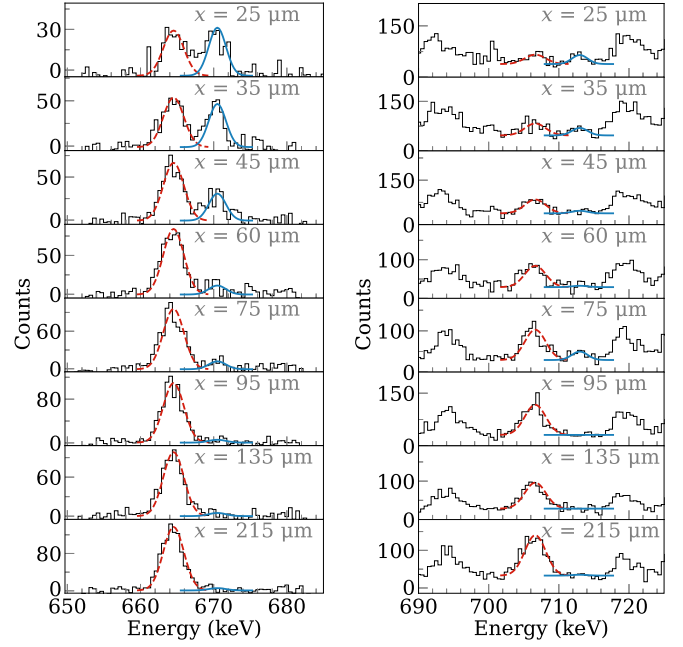


FIG. 2. Spectra of the $15/2^- \rightarrow 11/2^-$ (left panel) and $19/2^- \rightarrow 15/2^-$ (right panel) transitions in ^{117}Te , obtained by gating on the shifted component of the respective direct feeding transition for eight different target-to-stopper distances x in $(R2, R2)$ and the summed matrix $(R2, R2) + (R1, R2)$, respectively. The shifted component is shown by the red dashed line, while the stopped component is shown by the blue continuous line. The spectra are background subtracted but not normalized.

the following formula[15,21]:

$$\tau(x) = \frac{\{C_s, A_u\}(x) - \langle \delta \rangle \{C_s, B_u\}(x)}{\frac{d}{dx}\{C_s, A_s\}(x)} \frac{1}{v}, \quad (2)$$

where $\langle \delta \rangle$ is the mean value of $\delta(x)$ and

$$\delta(x) = \frac{\{C_s, A_u\}(x) + \{C_s, A_s\}(x)}{\{C_s, B_u\}(x) + \{C_s, B_s\}(x)}. \quad (3)$$

In Eqs. (2) and (3), C denotes the indirect gate on the $23/2^- \rightarrow 19/2^-$ transition, B denotes the direct feeding $19/2^- \rightarrow 15/2^-$ transition, and A denotes the depopulating $15/2^- \rightarrow 11/2^-$ transition. The contribution of the 718 keV doublets, while gating on the $23/2^- \rightarrow 19/2^-$ transition, was found to be negligible by comparing with the intensity of nearby transitions; thus they did not affect the analysis of the $19/2^-$ state lifetime.

As with the analysis of the $19/2^- \rightarrow 15/2^-$ transition in ^{117}Te , the gating was carried out in both matrices $(R2, R2)$ and $(R1, R2)$ and the resulting background-subtracted projections were added to increase statistics before the fitting was performed. It should be noted that, even with adding the matrices, the statistics in the ^{119}Te peaks were still lower than in the case of ^{117}Te , making it more sensitive to the background subtraction and subsequent fitting. This is reflected in a larger statistical error. Furthermore, the statistics were not enough to perform the analysis in the summed matrix $(R2, R1) + (R1, R1)$.

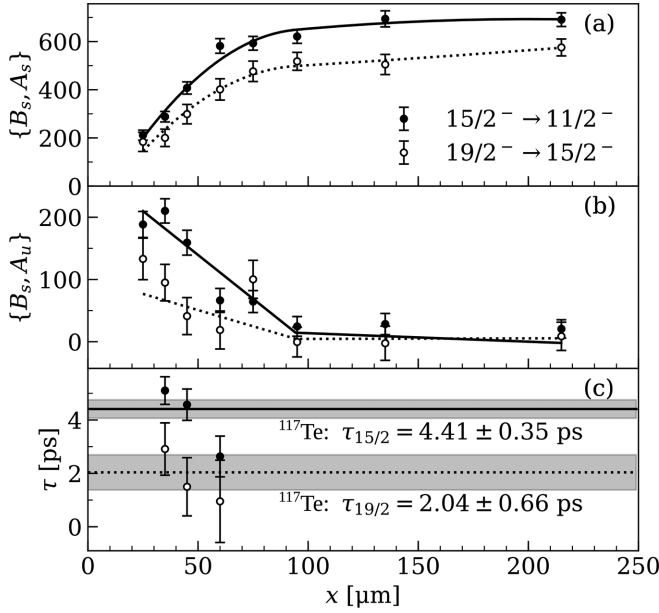


FIG. 3. Determination of the lifetime of the $15/2^-$ and $19/2^-$ states in ^{117}Te using coincidence matrix $(R2, R2)$ and summed matrix $(R2, R2) + (R1, R2)$, respectively. The gate is set on the shifted $19/2^- \rightarrow 15/2^-$ and $23/2^- \rightarrow 19/2^-$ transitions (B_s), respectively. (a) Intensity of the shifted $15/2^- \rightarrow 11/2^-$ and $19/2^- \rightarrow 15/2^-$ transitions (A_s). The solid line shows the fit performed in NAPATAU. (b) Intensity of the unshifted component (A_u). The solid line is constructed by multiplying the deduced mean lifetime τ with the derivative of the fitted line in (a) and the mean velocity. (c) Lifetimes calculated in the region of sensitivity 35–60 μm). The gray regions mark the boundaries for the standard error of the weighted mean.

The results of the fitting are displayed in Fig. 4 and the results of the DDCM analysis in Figs. 5 and 6 for the lifetimes of the $15/2^-$ and $19/2^-$ states, respectively.

C. Results

From the lifetime the reduced transition probability, $B(E2)$, can be calculated in Weisskopf units (W.u.) as

$$B(E2 \downarrow) = \frac{1.377 \times 10^4}{E_\gamma^5 A^{4/3} \tau (1 + \alpha)} \text{ W.u.}, \quad (4)$$

where E_γ is the energy of the transition in MeV, τ is the lifetime in ps, and the internal conversion coefficient α is taken from Refs. [23,24]. A summary of the experimental lifetimes obtained in the present study for the $15/2^-$ and $19/2^-$ states in both ^{117}Te and ^{119}Te , together with deduced $B(E2)$ values, are given in Table I. The weighted average values are calculated and the standard error is determined. Only statistical uncertainties were considered in the analysis.

IV. DISCUSSION

The new lifetime values for ^{117}Te and the remeasured values in ^{119}Te presented in Table I add further puzzle pieces to the study of the structure of the ground-state band in Te nuclei. With the trend of the transition strengths in even-even

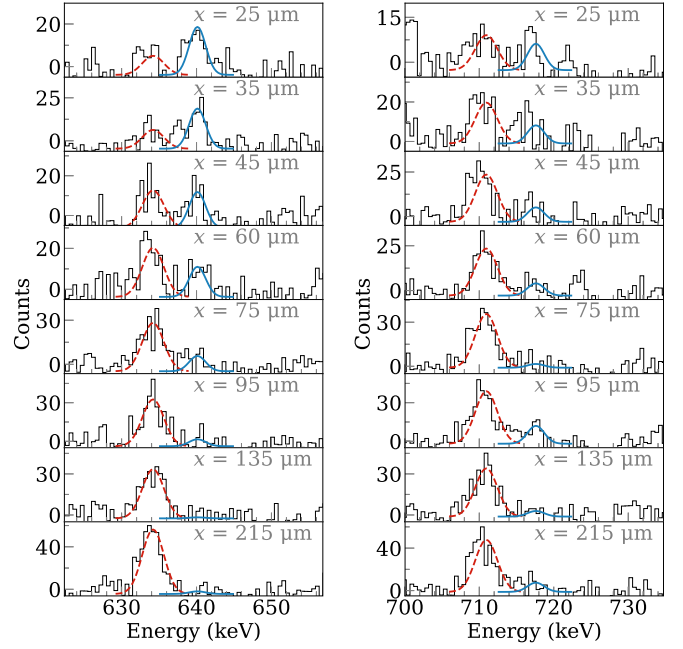


FIG. 4. Spectra of the $15/2^- \rightarrow 11/2^-$ (left panel) and $19/2^- \rightarrow 15/2^-$ (right panel) transitions in ^{119}Te , obtained by gating on the shifted component of the respective direct feeding transition for eight different target-to-stopper distances x in the summed matrix $(R2, R2) + (R1, R2)$. The shifted component is shown by a red dashed line, while the stopped component is shown by a blue continuous line. The spectra are background subtracted, but not normalized.

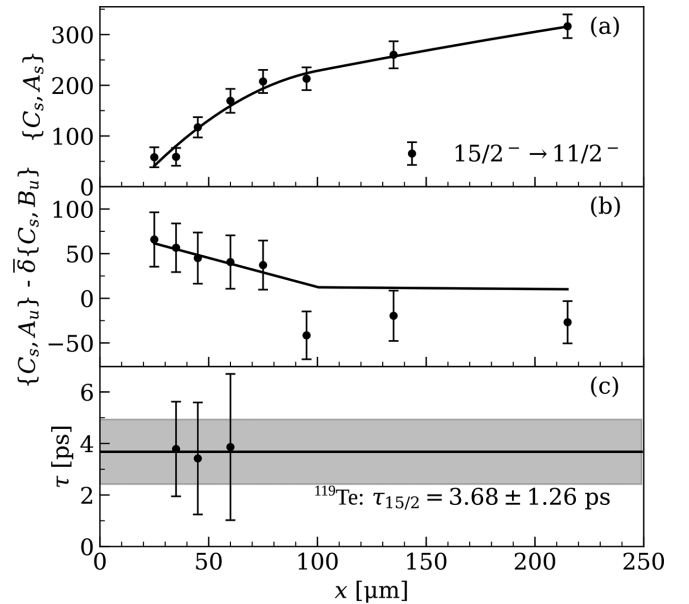


FIG. 5. Determination of the lifetime of the $15/2^-$ state in ^{119}Te using summed coincidence matrix $(R2, R2) + (R1, R2)$. The details are similar to those in Fig. 3, except in (b), where the differences between A_u and B_u are plotted (see text for details). Here, transitions A, B, and C are the $15/2^- \rightarrow 11/2^-$, $19/2^- \rightarrow 15/2^-$, and $23/2^- \rightarrow 19/2^-$ transitions, respectively.

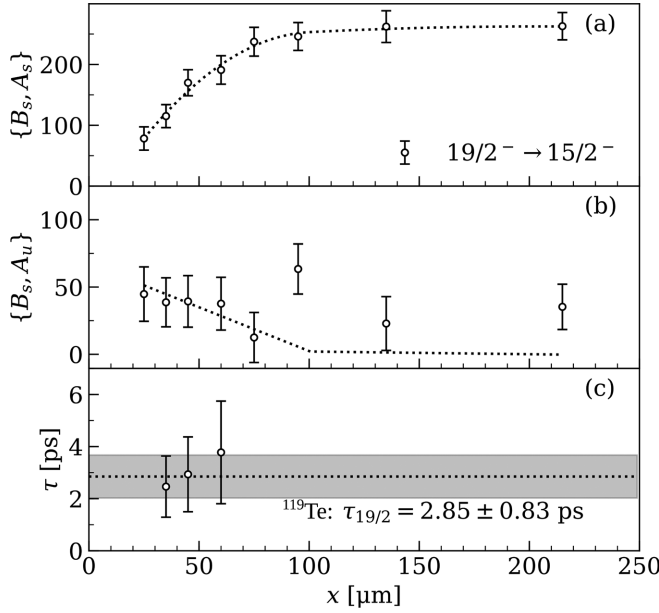


FIG. 6. Determination of the lifetime of the $19/2^-$ state in ^{119}Te using summed coincidence matrix $(R2, R2) + (R1, R2)$. The details are the same as in Fig. 3, except here transitions A and B are the $19/2^- \rightarrow 15/2^-$ and $23/2^- \rightarrow 19/2^-$ transitions, respectively.

midshell Te nuclei only just recently pinned down, and the new odd- A measurements presented in this work, there is good opportunity to more closely study the systematics of the reduced transition probabilities over the Te isotopic chain.

In Fig. 7(a) the known reduced transition probabilities of the $2^+ \rightarrow 0^+$ and $4^+ \rightarrow 2^+$ transitions, and their counterparts in the $\nu h_{11/2}$ band, are plotted for all Te isotopes up to the shell closure at $A = 134$. The $B(E2; 2^+ \rightarrow 0^+)$ values for the even-even nuclei resemble the expected parabolic shape, but with the maximum shifted slightly from the midshell at $N = 66$ to $N = 68$ and an asymmetry caused by the enhancement of the values with $N < 66$. This enhancement has been attributed to an increased neutron-proton correlation closer to the shell closure at $N = 50$ [25]. In the odd- A isotopes, the values of

TABLE I. Experimental results and weighted average of the lifetime τ for both the $15/2^-$ and the $19/2^-$ states. The $B(E2)$ values in Weisskopf units are also given.

Nucleus	$J_i^\pi \rightarrow J_f^\pi$	Rings (gate, fit)	τ_{exp} (ps)	$B(E2)$ (W.u.)
^{117}Te	$15/2^- \rightarrow 11/2^-$	(R2, R2)	4.41(35)	
		(R2, R1)	6.49(82)	
		(R1, R2)	3.46(47)	
		(R1, R1)	3.57(70)	
		average	4.23(48)	42_{-4}^{+5}
	$19/2^- \rightarrow 15/2^-$	(R1, R2) + (R2, R2)	2.04(66)	
	(R1, R1) + (R2, R1)	1.98(99)		
	average	2.02(55)	64_{-14}^{+24}	
^{119}Te	$15/2^- \rightarrow 11/2^-$	(R1, R2) + (R2, R2)	3.7(13)	59_{-15}^{+30}
	$19/2^- \rightarrow 15/2^-$	(R1, R2) + (R2, R2)	2.85(83)	43_{-10}^{+18}

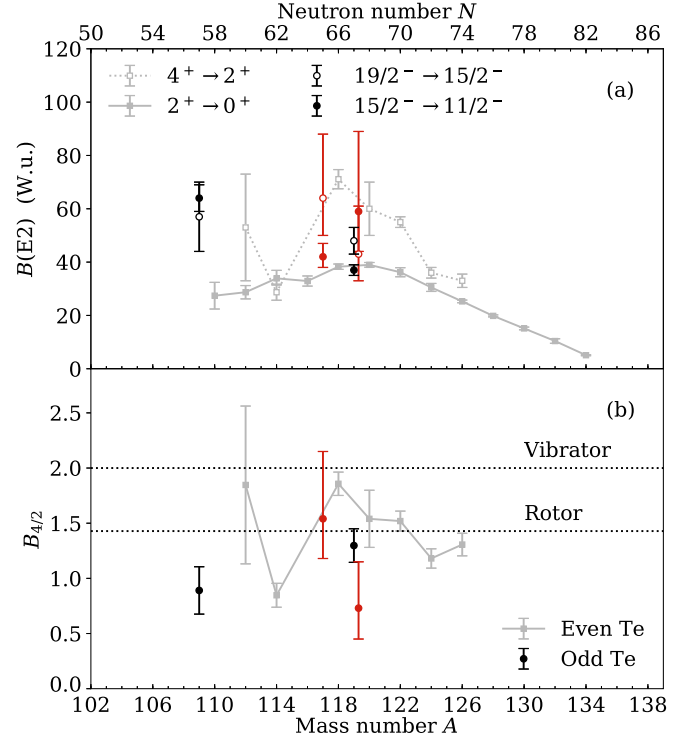


FIG. 7. (a) Reduced transition probabilities in the tellurium isotopic chain. Data are taken from Refs. [7,8,10,11,26–31] (black and gray) and the present work (red). Note that the values for ^{119}Te found in this work have been shifted slightly on the x axis for clarity. (b) Ratio of the reduced transition probabilities in (a); see text for details. Dotted line signals the benchmark values for perfect vibrators and rotors.

$B(E2; 15/2^- \rightarrow 11/2^-)$ presented in this work for ^{117}Te and ^{119}Te , together with the previous measurement of ^{109}Te , seem to suggest systematically higher values than the corresponding transition strength in the neighboring even-even core. In particular, ^{109}Te is greatly enhanced as compared to its neighbors. It was suggested in Ref. [10] that this enhancement is also due to the enhanced neutron-proton correlation when nearing the $N = 50$ shell closure.

As for the second excited state, the $B(E2; 4^+ \rightarrow 2^+)$ values follow a similar parabolic shape as the $B(E2; 2^+ \rightarrow 0^+)$, but with a sudden drop at $A = 114$. This sharp drop of the $B(E2; 4^+ \rightarrow 2^+)$ value, causing an unusually small $B_{4/2}$ ratio in a nucleus far from the closed shell, is also seen for the even—even nuclei at $A = 114$ in the Sn and Xe isotopic chains (see Figs. 1 and 7 in Ref. [32]). The $B(E2; 19/2^- \rightarrow 15/2^-)$ values on the other hand, seem to be on a similar level as compared to the transition strengths in the even-even neighbors, with no sharp drops. It was suggested in Ref. [32] that there may exist a critical limit in the Te, Xe, and Sn nuclei, where the $B_{4/2}$ ratio drops below 1 for $A \leq 114$. However, no explanation for why this critical limit exists is offered. This critical limit is also tentatively contradicted by the low $B_{4/2}$ value for ^{119}Te reported in this work. To further test this hypothesis, a measurement of, e.g., the lifetime of the 4^+ state in ^{110}Te and ^{116}Te would be of great interest.

It should be noted, however, that while the $B(E2; 19/2^- \rightarrow 15/2^-)$ of ^{119}Te measured in this work is in agreement with the previous measurement of ^{119}Te , the $B(E2; 15/2^- \rightarrow 11/2^-)$ value measured in Ref. [11] is lower, closer to the $B(E2; 2^+ \rightarrow 0^+)$ values of the even- A Te nuclei in the region. Using the values measured in that work the $B_{4/2}$ ratio of ^{119}Te is closer to that of a rotor, with $B_{4/2} = 1.30(15)$. In Ref. [11] the lifetimes in ^{119}Te were determined using RDDS and DDCM, as in this work. In that work, for the $15/2^- \rightarrow 11/2^-$ transition, the gate in Ref. [11] was set on the direct feeding transition of $19/2^- \rightarrow 15/2^-$. As explained above, in the present work the direct gate method was intentionally avoided in this particular case, due to the risk of contamination by the doublet in ^{119}Te with the same energy. This difference in method could possibly explain the slight difference in $B(E2; 15/2^- \rightarrow 11/2^-)$ values between Ref. [11] and this work.

In Fig. 7(b) the $B_{4/2}$ ratios in Te are plotted together with the benchmarks for a pure vibrator ($B_{4/2} = 2$) and rotor ($B_{4/2} = 10/7$). It is clear from the figure that most Te isotopes fall below the vibrational limit. This result is contrasted by the highly vibrational-like energy ratios ($E_{4/2} \approx 2-2.2$) found in all even and odd Te nuclei up to $N \approx 78$. It is also interesting to note that there are now potentially three Te nuclei with $B_{4/2} < 1$ and $E_{4/2} > 2$: ^{109}Te , ^{114}Te , and ^{119}Te . This so-called $B_{4/2}$ anomaly rarely happens in open shell nuclei across the nuclear chart. In addition to the Te nuclei, it has so far only been observed in $^{108,112,114}\text{Sn}$ [33–36], ^{114}Xe [37], ^{166}W [38], $^{168,169,170}\text{Os}$ [39–41], and ^{172}Pt [42]. The new measurements presented in this work indicate that it might occur systematically in the Te isotopes, which is even more dramatic as the nuclei were long expected to be vibrational.

These low $B_{4/2}$ values cannot be explained by microscopic calculations within LSSM or beyond mean field model approaches. By using the framework of the geometric interacting boson model (IBM), however, it has recently been proposed that the anomaly can be due to the effect of triaxial deformation, and may be enhanced in the phase transition from vibration to rotation [43–45]. There are some indications that the even-even isotopes $^{114,118}\text{Te}$ may show rather soft triaxial deformation, such as the low excitation energy of the 0_2^+ state in ^{118}Te (cf. Fig. 59 in [5]). Therefore, total Routhian surface (TRS) [46] calculations have been done in this work for the lowest spin states in nuclei $^{117,119}\text{Te}$ and neighboring even-even Te isotopes with the deformed Woods-Saxon potential. The results are very similar for both ^{117}Te and ^{119}Te . A representative example of the energy contour for the $\nu h_{11/2}$ band at low spin is shown in Fig. 8. The calculations reveal an unusually soft triaxiality in $^{117,119}\text{Te}$, with a prolate and a triaxial minimum at approximately the same energy, which is consistent with other types of mean field calculations.

In order to further study the structure and collective properties of $^{117,119}\text{Te}$ and the neighboring even-even nucleus ^{118}Te , both LSSM and IBM calculations have been performed. The LSSM calculations were done in the $0g_{7/2}1d_{5/2}1d_{3/2}2s_{1/2}0h_{11/2}$ model space including all proton and neutron orbitals between $N/Z = 50$ and 82 with the same effective Hamiltonian and effective charges as in Ref. [25].

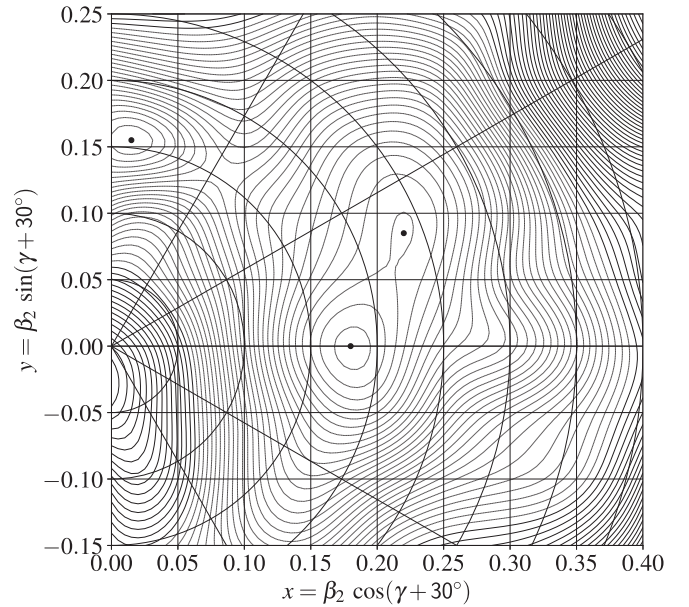


FIG. 8. TRS calculations for ^{119}Te at $\hbar\omega = 0.30$ MeV. The energy difference between neighboring contour lines is 0.10 MeV. The three minima are located at $(\beta_2, \gamma, E_{\text{Routhian}}, I_x) = (0.18, -30.0^\circ, -2.84 \text{ MeV}, 10.1\hbar)$, $(0.24, -8.9^\circ, -2.61 \text{ MeV}, 10.4\hbar)$, and $(0.15, 54.5^\circ, -2.19 \text{ MeV}, 16.1\hbar)$. The calculations were made with self-consistent pairing and for the following β_4 values: $-0.10, -0.05, 0.0, 0.05, 0.1$. The Routhian was minimized with respect to β_4 .

The full configuration interaction calculation for $^{117-119}\text{Te}$ is at the very limit of the LSSM capability. In the practical calculations, the dimension of the Hamiltonian matrix was limited to around 2×10^9 by imposing a monopole truncation technique [47,48], firstly due to the limited computational resource available at this stage, but also by considering the possibility to evaluate states beyond the yrast band. The lowest few states with spin values 0, 2, 4, and 6 were calculated for the even-even nucleus ^{118}Te and with spin values 11/2, 15/2, 19/2, and 23/2 for $^{117,119}\text{Te}$. The calculated energy levels are displayed in Fig. 1. The LSSM calculations reproduce perfectly not only the nearly identical vibrational-like behavior of the yrast band but also the excitation energies of the yrare states (not shown in Fig. 1) which also follow the predictions of the ideal vibrator, except that the energies of the 6^+ and corresponding $23/2^-$ state seem a bit too low (partly due to the reason that they seem to converge slowly as a function of the model space dimension in the truncated calculation). The main concern is, however, that the calculated $B(E2)$ properties for the three nuclei $^{117-119}\text{Te}$ have quite similar behavior with $B_{4/2} \approx 1.4$, i.e., a quantity that is closer to a quantum rotor. In other words, in the LSSM picture the odd neutron in the $h_{11/2}$ orbital behaves more or less like a spectator weakly coupled to the collective ^{118}Te core in the complex shell model wave functions. A similar conclusion was obtained for lighter Te isotopes [10]. It should be mentioned that, unlike rotational collectivity, the microscopic origin of vibration is not yet understood from the shell model perspective. In other words, it is not clear which part of the effective interaction can lead to nuclear vibration. The measurements published here not

TABLE II. Summary of experimental and theoretical $B_{4/2}$ ratios. Experimental values for ^{117}Te and ^{119}Te taken from this work and for ^{118}Te it is taken from the weighted average of the values reported in Refs. [7,8,28].

Nucleus	$B_{4/2}$		
	Expt.	LSSM	IBM
^{117}Te	$1.54^{+0.61}_{-0.36}$	1.22	1.46
^{118}Te	1.86(10)	1.35	1.91
^{119}Te	$0.73^{+0.42}_{-0.28}$	1.32	1.06

only challenge the commonly believed vibrational nature of these states, but also the underlying effective interaction in the microscopic shell model.

The IBM calculations were performed with an effective Hamiltonian in the form [43–45]

$$H = a_1 \hat{n}_d + a_2 [\hat{Q} \cdot \hat{Q}] + a_3 H_3 + a_4 [\hat{Q} \cdot \hat{q}_F], \quad (5)$$

where the first two terms describe the nuclear vibration and rotation. The H_3 term denotes higher-order terms that may lead to a mixture among vibration and rotation as well as nuclear triaxial deformation, for which only the term $L \times Q \times L$ is considered in this work for simplicity. In the present work, the parameters of these terms are fitted to the spectra of $^{116,118}\text{Te}$. The $[\hat{Q} \cdot \hat{q}_F]$ term describes the interaction with the odd neutron particle (or hole) for which the parameter is adjusted for a better reproduction of the properties of $^{117,119}\text{Te}$. As one would expect, since the spectra of ^{118}Te and the odd- A $^{117,119}\text{Te}$ are very vibrational-like, the Hamiltonian thus determined is dominated by the contribution from the vibrational n_d term. As a result, similar to those of the shell model, the IBM calculations predict rather vibrational behavior for the isotopes $^{117-119}\text{Te}$. By enhancing the $[\hat{Q} \cdot \hat{q}_F]$ term the $B_{4/2}$ ratio can be reduced, in order to tune the values to the experimental results. It is emphasized that, as shown in Refs. [43–45], a significant reduction of the $B_{4/2}$ value may be expected for a certain range of H_3 values, together with the $[\hat{Q} \cdot \hat{q}_F]$ interaction for odd- A systems, in connection to the onset of triaxial deformation and triaxial softness. This is consistent with the TRS calculations as plotted in Fig. 8.

In Table II a summary of the experimental and calculated LSSM and IBM $B_{4/2}$ values is presented for $^{117-119}\text{Te}$. As discussed above, while the energy ratio $E_{4/2}$ exhibits near perfect vibrational-like behavior for all three of these midshell

region nuclei, the three experimental $B_{4/2}$ values suggest three different behaviors. While ^{118}Te is near vibrational, ^{117}Te is closer to rotational and the value for ^{119}Te is, tentatively, unexpectedly low.

V. CONCLUSION

Lifetimes of the $15/2^-$ and $19/2^-$ states have been measured in ^{117}Te and remeasured in ^{119}Te for the first time, by using the RDDS technique and the coincidence DDC method. Comparison to systematics in even-even neighbors shows that the extracted transition strengths in ^{117}Te and ^{119}Te seem to follow the same trend. However, the $B_{4/2}$ ratios for those two nuclei are smaller than that of ^{118}Te . Especially surprising is the small value of ^{119}Te found in this work. This tentatively adds ^{119}Te to the growing list of exotic collective nuclei far from closed shells, with $E_{4/2} > 2$ but $B_{4/2} < 1$. The results were compared with LSSM and IBM calculations. While both models reproduce well the energy spectra of those nuclei, the shell model cannot fully reproduce the observed anomalous $B_{4/2}$ feature. By tuning the strength for the Fermion-boson interaction or the higher-order term of IBM it is possible to replicate the experimental results. One may need more data to fully pin down those parameters, but this calculation suggests that the odd- A isotopes are triaxially soft, which is consistent with TRS calculations.

ACKNOWLEDGMENTS

This work was supported by the EU HORIZON2020 programme ‘‘Infrastructures,’’ Project No. 654002 (ENSAR2). C.Q. acknowledges the computational resources provided by the National Academic Infrastructure for Supercomputing in Sweden (NAISS) at PDC, KTH and support from the Olle Engkvist Foundation. B.S.N.S. would like to acknowledge the financial support of the UKRI STFC through Grants No. ST/T001739/1 and No. ST/P005101/1.

DATA AVAILABILITY

The data that support the findings of this article are not publicly available upon publication because it is not technically feasible and/or the cost of preparing, depositing, and hosting the data would be prohibitive within the terms of this research project. The data are available from the authors upon reasonable request.

- [1] J. Kern, P. E. Garrett, J. Jolie, and H. Lehmann, Search for nuclei exhibiting the U(5) dynamical symmetry, *Nucl. Phys. A* **593**, 21 (1995).
- [2] P. E. Garrett, J. L. Wood, and S. W. Yates, Critical insights into nuclear collectivity from complementary nuclear spectroscopic methods, *Phys. Scr.* **93**, 063001 (2018).
- [3] K. Heyde and J. L. Wood, Shape coexistence in atomic nuclei, *Rev. Mod. Phys.* **83**, 1467 (2011).
- [4] P. E. Garrett, M. Zielińska, and E. Clément, An experimental view on shape coexistence in nuclei, *Prog. Part. Nucl. Phys.* **124**, 103931 (2022).
- [5] S. Leoni, B. Fornal, A. Bracco, Y. Tsunoda, and T. Otsuka, Multifaceted character of shape coexistence phenomena in atomic nuclei, *Prog. Part. Nucl. Phys.* **139**, 104119 (2024).
- [6] F. von Spee, M. Beckers, A. Blazhev, A. Dewald, F. Dunkel, A. Esmaylzadeh, C. Fransen, G. Hackenberg, J. Jolie, L. Knafila, C. D. Lakenbrink, M. Schiffer, N. Warr, and M. Weinert, Structure of low-lying states in ^{116}Te , *Phys. Rev. C* **109**, 024325 (2024).
- [7] C. B. Li *et al.*, Lifetime measurements of the first 2^+ states in $^{116,118}\text{Te}$, *Phys. Rev. C* **109**, 034310 (2024).

- [8] E. A. Cederlöf *et al.*, Lifetime measurement of the yrast 2^+ state in ^{118}Te , *Eur. Phys. J. A* **59**, 300 (2023).
- [9] A. Bohr and B. R. Mottelson, *Nuclear Structure, Vol. II* (World Scientific Publishing, Singapore, 1998).
- [10] M. G. Procter *et al.*, Electromagnetic transition strengths in ^{109}Te , *Phys. Rev. C* **86**, 034308 (2012).
- [11] D. Bucurescu *et al.*, The ROSPHERE γ -ray spectroscopy array, *Nucl. Instrum. Methods Phys. Res. Sect. A* **837**, 1 (2016).
- [12] C. B. Moon, S. J. Chae, T. Komatsubara, T. Shizuma, Y. Sasaki, H. Ishiyama, T. Jumatsu, and K. Furuno, Collective and noncollective states in ^{117}Te , *Nucl. Phys. A* **657**, 251 (1999).
- [13] C. Papadopoulos, R. Vlastou, M. Serris, H. G. Hartas, N. Fotiades, C. A. Kalfas, S. Harissopoulos, S. Kossionides, J. Simpson, E. S. Paul, S. Araddad, C. W. Beausang, M. A. Bentley, M. J. Joyce, and J. F. Sharpey-Schafer, High spin levels in ^{119}Te , *Z. Phys. A* **352**, 243 (1995).
- [14] T. K. Alexander and J. S. Forster, Lifetime measurements of excited nuclear levels by Doppler-Shift methods, in *Advances in Nuclear Physics: Volume 10*, edited M. Baranger and E. Vogt (Springer, Boston, MA, 1978), pp. 197–331.
- [15] A. Dewald, O. Möller, and P. Petkov, Developing the Recoil Distance Doppler-Shift technique towards a versatile tool for lifetime measurements of excited nuclear states, *Prog. Part. Nucl. Phys.* **67**, 786 (2012).
- [16] M. J. Taylor *et al.*, A new differentially pumped plunger device to measure excited-state lifetimes in proton emitting nuclei, *Nucl. Instrum. Methods Phys. Res. Sect. A* **707**, 143 (2013).
- [17] C. W. Beausang and J. Simpson, Large arrays of escape suppressed spectrometers for nuclear structure experiments, *J. Phys. G* **22**, 527 (1996).
- [18] F. A. Beck, EUROBALL: Large gamma ray spectrometers through european collaborations, *Prog. Part. Nucl. Phys.* **28**, 443 (1992).
- [19] J. Pakarinen *et al.*, The JUROGAM 3 spectrometer, *Eur. Phys. J. A* **56**, 149 (2020).
- [20] P. Rahkila, Grain—A Java data analysis system for Total Data Readout, *Nucl. Instrum. Methods Phys. Res. Sect. A* **595**, 637 (2008).
- [21] A. Dewald, S. Harissopoulos, and P. von Brentano, The differential plunger and the differential decay curve method for the analysis of recoil distance Doppler-shift data, *Z. Phys. A* **334**, 163 (1989).
- [22] B. Saha, Bestimmung der Lebensdauer kollektiver Kernanregungen in ^{124}Xe und Entwicklung von entsprechender Analysesoftware, Ph.D. thesis, Universität zu Köln, 2004, <https://kups.uni-koeln.de/1246/>.
- [23] T. Kibédi, T. W. Burrows, M. B. Trzhaskovskaya, P. M. Davidson, and C. W. Nestor, Jr., Evaluation of theoretical conversion coefficients using BrIcc, *Nucl. Instrum. Methods Phys. Res. Sect. A* **589**, 202 (2008).
- [24] BrIcc conversion coefficient calculator, <https://bricc.anu.edu.au/>.
- [25] C. Qi, The anomalous quadrupole collectivity in Te isotopes, *Phys. Rev. C* **94**, 034310 (2016).
- [26] B. Pritychenko, M. Birch, B. Singh, and M. Horoi, Tables of E2 transition probabilities from the first 2^+ states in even-even nuclei, *At. Data Nucl. Data Tables* **107**, 1 (2016).
- [27] D. A. Testov *et al.*, Octupole correlations near ^{110}Te , *Phys. Rev. C* **103**, 044321 (2021).
- [28] A. A. Pasternak, J. Srebrny, A. D. Efimov, V. M. Mikhajlov, E. O. Podsvirova, C. Droste, T. Morek, S. Juutinen, G. B. Hagemann, M. Piiparinen, S. Törmänen, and A. Virtanen, Lifetimes in the ground-state band and the structure of ^{118}Te , *Eur. Phys. J. A* **13**, 435 (2002).
- [29] M. Doncel *et al.*, Spin-dependent evolution of collectivity in ^{112}Te , *Phys. Rev. C* **96**, 051304(R) (2017).
- [30] O. Möller, N. Warr, J. Jolie, A. Dewald, A. Fitzler, A. Linnemann, K. O. Zell, P. E. Garrett, and S. W. Yates, E2 transition probabilities in ^{114}Te : A conundrum, *Phys. Rev. C* **71**, 064324 (2005).
- [31] M. Saxena, R. Kumar, A. Jhingan, S. Mandal, A. Stolarz, A. Banerjee, R. K. Bhowmik, S. Dutt, J. Kaur, V. Kumar, M. M. Mbaye, V. R. Sharma, and H. J. Wollersheim, Rotational behavior of $^{120,122,124}\text{Te}$, *Phys. Rev. C* **90**, 024316 (2014).
- [32] C. Müller-Gatermann, A. Dewald, C. Fransen, M. Beckers, A. Blazhev, T. Braunroth, A. Goldkuhle, J. Jolie, L. Kornwebel, W. Reviol, F. Von Spee, and K. O. Zell, Evolution of collectivity in ^{118}Xe , *Phys. Rev. C* **102**, 064318 (2020).
- [33] M. Siciliano *et al.*, Pairing-quadrupole interplay in the neutron-deficient tin nuclei: First lifetime measurements of low-lying states in $^{106,108}\text{Sn}$, *Phys. Lett. B* **806**, 135474 (2020).
- [34] A. Kundu *et al.*, New lifetime measurement for the 2^+ level in ^{112}Sn by the Doppler-shift attenuation method, *Phys. Rev. C* **103**, 034315 (2021).
- [35] N.-G. Jonsson, A. Bäcklin, J. Kantele, R. Julin, M. Luontama, and A. Passoja, Collective states in even Sn nuclei, *Nucl. Phys. A* **371**, 333 (1981).
- [36] J. Gableske, A. Dewald, H. Tiesler, M. Wilhelm, T. Klemme, O. Vogel, I. Schneider, R. Peusquens, S. Kasemann, K. Zell, P. von Brentano, P. Petkov, D. Bazzacco, C. Rossi Alvarez, S. Lunardi, G. de Angelis, M. de Poli, and C. Fahlander, Collectivity of the intruder bands in ^{114}Sn , *Nucl. Phys. A* **691**, 551 (2001).
- [37] G. de Angelis *et al.*, Coherent proton–neutron contribution to octupole correlations in the neutron-deficient ^{114}Xe nucleus, *Phys. Lett. B* **535**, 93 (2002).
- [38] B. Saygi *et al.*, Reduced transition probabilities along the yrast line in ^{166}W , *Phys. Rev. C* **96**, 021301 (2017).
- [39] T. Grahn *et al.*, Excited states and reduced transition probabilities in ^{168}Os , *Phys. Rev. C* **94**, 044327 (2016).
- [40] W. Zhang *et al.*, Lifetime measurements of excited states in $^{169,171,173}\text{Os}$: Persistence of anomalous $B(E2)$ ratios in transitional rare earth nuclei in the presence of a decoupled $i_{13/2}$ valence neutron, *Phys. Lett. B* **820**, 136527 (2021).
- [41] A. Goasduff, J. Ljungvall, T. R. Rodríguez, F. L. B. Garrote, A. Etile, G. Georgiev, F. Giacoppo, L. Grente, M. Klintefjord, A. Kuşoğlu, I. Matea, S. Rocca, M.-D. Salsac, and C. Sotty, $B(E2)$ anomalies in the yrast band of ^{170}Os , *Phys. Rev. C* **100**, 034302 (2019).
- [42] B. Cederwall *et al.*, Lifetime measurements of excited states in ^{172}Pt and the variation of quadrupole transition strength with angular momentum, *Phys. Rev. Lett.* **121**, 022502 (2018).
- [43] Y. Zhang, Y. W. He, D. Karlsson, C. Qi, F. Pan, and J. P. Draayer, A theoretical interpretation of the anomalous reduced E2 transition probabilities along the yrast line of neutron-deficient nuclei, *Phys. Lett. B* **834**, 137443 (2022).
- [44] Y. Zhang, S.-N. Wang, F. Pan, C. Qi, and J. P. Draayer, Triaxial rotor modes in finite- N boson systems, *Phys. Rev. C* **110**, 024303 (2024).

- [45] T. Teng, Y. Zhang, and C. Qi, A novel approach for the anomalous collectivity in neutron-deficient Os isotopes, *Chin. Phys. C* **49**, 014102 (2025).
- [46] R. Wyss, J. Nyberg, A. Johnson, R. Bengtsson, and W. Nazarewicz, Highly deformed intruder bands in the $A \approx 130$ mass region, *Phys. Lett. B* **215**, 211 (1988).
- [47] P. Choudhary and C. Qi, Monopole and seniority truncations in the large-scale configuration interaction shell model approach, *Symmetry* **16**, 1685 (2024).
- [48] C. Qi, L. Y. Jia, and G. J. Fu, Large-scale shell-model calculations on the spectroscopy of $N < 126$ Pb isotopes, *Phys. Rev. C* **94**, 014312 (2016).